NO_3 Yield in the $O(^3P) + BrONO_2$ Reaction

James B. Burkholder*

Aeronomy Laboratory, National Oceanic and Atmospheric Administration, 325 Broadway, Boulder, Colorado 80303

Received: December 7, 1999; In Final Form: April 3, 2000

The NO_3 product yield in the reaction $O(^3P) + BrONO_2$ was measured to be >0.85 at 298 K. Yield measurements were made using the technique of laser-pulsed photolysis with long-path transient absorption detection of NO_3. $O(^3P)$ atoms were produced in the presence of $BrONO_2$ by the 248-nm photolysis of O_3 in a N_2 bath gas. The photolysis laser fluence was calibrated using N_2O_5 as an actinometer.

Introduction

Soller et al.[1] have recently reported rate coefficient measurements for the reaction

$$O(^3P) + BrONO_2 \rightarrow \text{Products} \qquad (1)$$

where $k_1(T) = 1.99 \times 10^{-11} \exp(205/T)$ cm^3 molecule $^{-1}$ s^{-1}. As described by Soller et al., reaction 1 represents a significant loss process relative to photolysis for $BrONO_2$ in the upper stratosphere. Reaction 1 is currently not included in recommendations for atmospheric modeling.[2] A number of energetically accessible product channels are available for reaction 1

$$\begin{array}{llrr} & & \Delta H\ (\text{kcal mol}^{-1}) & \\ O(^3P) + BrONO_2 & \rightarrow BrNO + O_3 & -17 & (1a) \\ & \rightarrow BrO + NO + O_2 & -19 & (1b) \\ & \rightarrow BrO + NO_3 & -23 & (1c) \\ & \rightarrow OBrO + NO_2 & -26 & (1d) \\ & \rightarrow Br + O_2 + NO_2 & -36 & (1e) \\ & \rightarrow BrOO + NO_2 & -37 & (1f) \\ & \rightarrow BrONO + O_2 & -45 & (1g) \\ & \rightarrow BrNO_2 + O_2 & -54 & (1h) \end{array}$$

where the thermochemical data used to calculate ΔH were taken from DeMore et al.[2] and Chase[3] (BrOO and OBrO). This list is based on energetics alone and includes reaction products that may not correlate with the reactants. To our knowledge, there are no studies of the products of reaction 1 reported in the literature.

The NO_3 yield in the $ClONO_2$ reaction

$$O(^3P) + ClONO_2 \rightarrow ClO + NO_3 \qquad (2)$$

has been measured to be near unity.[4] Therefore, by analogy, we expect channel (1c), $BrO + NO_3$, to be a major product channel for reaction 1. In this study, we have examined the products of reaction 1 using the technique of laser pulsed photolysis with long-path transient absorption detection of NO_3.

Experimental Section

The NO_3 product yield from reaction 1 was measured by producing a known concentration of O atoms via the pulsed-laser photolysis of O_3 in the presence of $BrONO_2$. The NO_3 temporal profile was measured quantitatively following the photolysis pulse by long-path (92-cm) diode laser transient absorption at 662 nm. The experimental apparatus and methods used are similar to those used in our recent study of the NO_3 product yield for reaction 2.[4,5] Therefore, only a brief overview of the details pertinent to the present study is provided below.

The concentrations of $BrONO_2$ and O_3 were measured directly in the reactor/absorption cell by UV absorption. Absorption measurements were made over the range 200−365 nm using a D_2 lamp and a 0.5-m spectrometer equipped with a diode array detector. $BrONO_2$ and O_3 concentrations were determined by fitting the measured spectrum using reference spectra recorded separately and literature cross sections.[2,6] Estimates of the possible Br_2O and Br_2 impurities in the $BrONO_2$ sample were also made from this analysis, with cross sections taken from Orlando and Burkholder[7] for Br_2O and Maric et al.[8] for Br_2.

A diode laser was used to monitor the formation of NO_3 by absorption following the photolysis pulse. The diode laser was nominally operated at the peak of the NO_3 absorption spectrum [662 nm, $\sigma(NO_3) = 2.23 \times 10^{-17}$ cm^2 [9]] and operated in single mode. The wavelength of the diode laser was stable to better than ±0.01 nm during all of the measurements. The intensity of the diode laser was stable to 2 parts in 10^5 over the duration of the measurements, 10 ms. The photolysis and diode laser beams co-propagated the full length of the reactor/absorption cell (92 cm). NO_3 absorption measurements were made by first recording the intensity of the diode laser before the photolysis laser pulse, taken to be I_0. The diode laser intensity after the photolysis laser pulse, I_t, was then used with I_0 to calculate the absorbance [$A = -\ln(I_t/I_0)$], as a function of time. In this system, NO_3 is the only species with significant absorption at 662 nm so that the calculated absorbance can be directly related to the NO_3 concentration.

Only a small photolysis laser fluence (in the reactor) was desired (i.e., low radical concentrations) to minimize secondary

---

* Correspondence should be sent to: James Burkholder, NOAA R/AL2, 325 Broadway, Boulder, CO 80303. E-mail: burk@al.noaa.gov.

10.1021/jp9942926 Published 2000 by the American Chemical Society

chemistry of the photolysis products. This was achieved by operating the photolysis laser at the minimum high voltage setting along with stacked neutral density filters (OD ~ 1) in the beam path. The laser fluence was measured to be $\sim 9 \times 10^{14}$ photon cm^{-2} (see calibration method below), which kept the fractions of O_3 and $BrONO_2$ photolyzed to less than 1% and 0.1%, respectively. The photolysis wavelength, 248 nm, was chosen over other possible excimer laser wavelengths (193, 308, and 351 nm) to minimize the amount of $BrONO_2$ photolysis relative to O_3.

$O(^1D)$ and $O(^3P)$ atoms were produced by the 248-nm photolysis of O_3

$$O_3 + h\nu \rightarrow O(^1D) + O_2 \tag{3a}$$

$$\rightarrow O(^3P) + O_2 \tag{3b}$$

The $O(^1D)$ atoms were quenched to ground-state $O(^3P)$ atoms within the first 0.1 μs by 100 Torr of N_2 bath gas

$$O(^1D) + N_2 \rightarrow O(^3P) + N_2 \tag{4}$$

where $k_4 = 2.6 \times 10^{-11}$ cm^3 $molecule^{-1}$ s^{-1} at 298 K.[2] Therefore, every photon absorbed by O_3 produced a ground-state O atom on a time scale faster than the subsequent O atom chemistry of interest.

The data used to determine the NO_3 yield in reaction 1 were acquired as follows. A D_2 lamp spectrum, I_0, was measured with only N_2 flowing through the reactor/absorption cell. O_3 and $BrONO_2$ were added to the N_2 flow, and a second spectrum, I, was recorded. The intensity of the diode laser beam exiting the reactor was measured. The photolysis laser was fired, and the diode laser intensity was recorded over the next 4 ms. Typically, 5−20 measurements were coadded to improve the signal-to-noise ratio of the measurement. The concentrations of O_3 and $BrONO_2$ were remeasured after the completion of the signal averaging and compared with the initial values. The concentrations typically agreed to better than 5%.

Laser Fluence Calibration. Determination of the NO_3 yield in reaction 1 requires an accurate determination of the initial O atom concentration, $[O]_0$. This initial O atom concentration was determined from the photolysis laser fluence and the concentration of ozone, $[O_3]$. The O_3 concentration was measured directly with the diode array spectrometer during the yield measurements. As used in our previous studies,[4,10] N_2O_5 photolysis

$$N_2O_5 + h\nu \rightarrow NO_2 + NO_3 \tag{5}$$

with NO_3 detection (as described above) was used for the laser fluence calibration measurements. The N_2O_5 actinometer was chosen to enable both the calibration and kinetic measurements to detect the same species, NO_3. This approach minimizes systematic errors in the calibration measurements due to such things as uncertainties in the NO_3 cross section.

The excimer laser fluence, LF in units of photon cm^{-2}, was determined from the slope of a plot of $[NO_3]$ vs $[N_2O_5]$

$$LF = [NO_3]/\{[N_2O_5]\ \sigma(N_2O_5)\ \Phi(NO_3)\} \tag{6}$$

where $[NO_3]$ is the NO_3 concentration produced by the laser pulse and $\sigma(N_2O_5)$ is the N_2O_5 absorption cross section at the photolysis wavelength (248 nm), 4.19×10^{-19} cm^2 $molecule^{-1}$. The NO_3 quantum yield, $\Phi(NO_3)$, for reaction 5 at 248 nm has been measured to be 0.80 ± 0.10.[4,11] The N_2O_5 concentration was measured by UV absorption using the diode array spectrometer. Each calibration consisted of measurements using at least five different N_2O_5 concentrations within the range $(0.3-3) \times 10^{15}$ molecule cm^{-3} at a total pressure of 100 Torr. A small correction, <5%, was applied to the calibration data to account for attenuation of the photolysis laser beam along the length of the reactor/absorption cell.

Materials. N_2O_5 was prepared in a slow flow by reacting excess O_3, from an ozonizer, with NO_2 at atmospheric pressure. NO_2 was prepared by reacting purified NO with excess O_2, which had been passed through a molecular sieve trap at dry ice temperature. NO_2 was collected in a dry-ice-cooled trap and purified by trap-to-trap distillation in an excess O_2 flow until a pure white solid remained. The N_2O_5 was trapped and stored at 195 K. N_2O_5 was introduced into the experimental chamber by passing a small N_2 flow through the trap. The temperature of the N_2O_5 trap was varied between 253 and 268 K during the calibration measurements.

$BrONO_2$ was synthesized by the reaction of BrCl with $ClONO_2$ using the method described by Spencer and Rowland[12] and used in our previous $BrONO_2$ UV/vis absorption cross-section study.[6] The $BrONO_2$ sample was stored in the dark at 195 K. $BrONO_2$ was added to the gas flow from its reservoir by flowing N_2 through the trap, which was maintained at temperatures in the range 240−250 K. $BrONO_2$ decomposes in the storage trap over a period of days, as indicated by the formation of Br_2. Any Br_2 that built up during the storage of the $BrONO_2$ sample was removed before the experiments by flowing N_2 through the trap while monitoring the UV absorption spectrum. The Br_2 impurity level was less than 5% during the NO_3 yield measurements. O_3 was stored in a silica gel trap at dry ice temperature and was introduced into the gas flow by passing a small N_2 flow through the trap.

N_2 (UHP, 99.9995%) was used as the buffer gas. The linear gas flow velocity in the absorption cell was ~10 cm s^{-1}. The reactor/absorption cell was flushed with a fresh gas mixture between laser pulses (0.08 Hz). All gases were mixed before they entered the reaction/absorption cell.

Results and Discussion

The NO_3 temporal profiles measured following photolysis of $BrONO_2/O_3$ gas mixtures are shown in Figure 1. The O_3 and $BrONO_2$ concentrations associated with each of these NO_3 profiles are given in Table 1. In general, the largest NO_3 concentrations are associated with the highest O_3 concentrations. The photolysis laser fluence used in these measurements was measured to be $(9.0 \pm 0.3) \times 10^{14}$ photon cm^{-2} using the methods described in the Experimental Section and taking $\Phi(NO_3) = 0.8$, eq 6. The quoted error limit is the 2σ error of the linear least-squares fit to the calibration data.

The NO_3 yield from reaction 1 was determined by fitting each of the NO_3 profiles shown in Figure 1 with the reaction mechanism outlined in Table 2. The majority of the reaction rate coefficients for the mechanism in Table 2 are well-known and were taken directly from the literature, as indicated. The exception is for the reaction

$$O + Br_2O \rightarrow \text{Products} \tag{7}$$

for which no kinetic data are available. The significance and uncertainties associated with this reaction are discussed below.

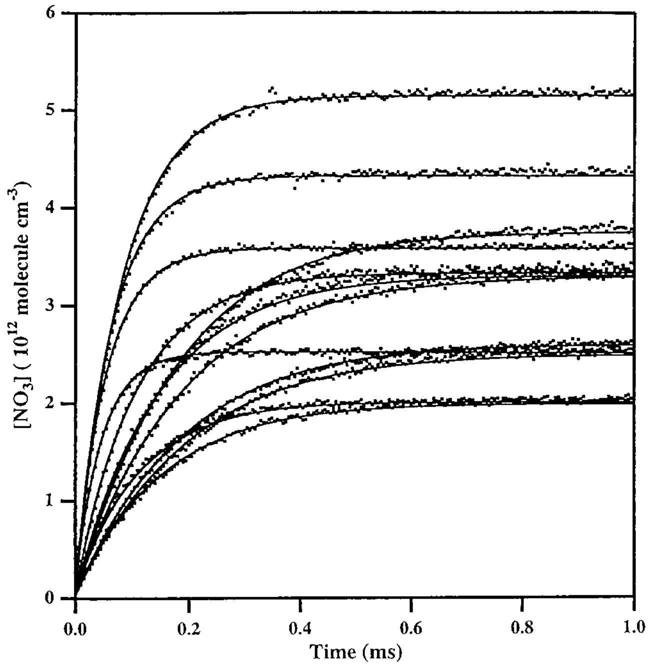

Figure 1. NO_3 concentration profiles measured (dots) following the photolysis of $BrONO_2/O_3/N_2$ gas mixtures at 298 K. The $BrONO_2$ and O_3 concentrations are given in Table 1. The solid lines represent the best fits to the data using the reaction mechanism given in Table 2, as discussed in the text.

TABLE 1: Experimental Concentrations and NO_3 Yields

$[BrONO_2]$ 10^{14} molecule cm^{-3}	$[O_3]$ 10^{14} molecule cm^{-3}	$[NO_3]$ yield
1.63	3.27	1.0
3.04	6.34	0.95
3.80	4.98	0.97
2.21	3.50	1.0
1.50	4.41	0.82
1.35	2.82	0.90
2.10	1.94	1.0
1.59	1.88	0.95
1.30	2.63	0.90
1.30	3.79	1.0
4.30	3.98	1.0
5.10	2.22	0.93

Also, data for the photolysis quantum yields for $BrONO_2$ at 248 nm

$$BrONO_2 + h\nu \rightarrow Br + NO_3 \tag{8a}$$

$$\rightarrow Br + NO_2 + O \tag{8b}$$

$$\rightarrow BrO + NO_2 \tag{8c}$$

$$\rightarrow BrO + NO + O \tag{8d}$$

is limited to two recent studies.[1,11] Harwood et al.[11] measured the NO_3 quantum yield (channel 8a), whereas Soller et al.[1] measured the Br (channels 8a and 8b) and O (channels 8b and 8d) atom yields. Combining the results from these two studies provides a reasonably good estimate of the quantum yields for the different channels (see Table 2). In this study, we have also performed $BrONO_2$ photolysis experiments (without O_3) to confirm the NO_3 quantum yield reported by Harwood et al.[11] and verify our methodology. In two measurements (Figure 2), we obtained an average value of $\Phi(NO_3) = 0.23$, in good agreement with the value of 0.28 ± 0.08 reported by Harwood et al.[11] Through an analysis of the increase in the concentration of NO_3 due to secondary chemistry (Table 2), these measurements also confirm the Br and O atom yields reported by Soller et al.[1] as discussed below.

TABLE 2: Reaction Mechanism Used in Data Analysis

reaction	rate coefficient[a] (298 K)	quantum yield	ref
$O_3 + h\nu \rightarrow O(^1D) + O_2$	–	0.90	2
$\rightarrow O(^3P) + O_2$	–	0.10	2
$BrONO_2 + h\nu \rightarrow Br + NO_3$	–	0.28	11
$\rightarrow Br + NO_2 + O$	–	0.07	1
$\rightarrow BrO + NO_2$	–	0.06	*b*
$\rightarrow BrO + NO + O$	–	0.59	1
$O(^1D) + N_2 \rightarrow O(^3P) + N_2$	2.6×10^{-11}		2
$O + BrONO_2 \rightarrow BrO + NO_3$	3.96×10^{-11}		1
$O + Br_2 \rightarrow BrO + Br$	1.4×10^{-11}		13
$O + O_3 \rightarrow O_2 + O_2$	8×10^{-15}		2
$O + Br_2O \rightarrow BrO + BrO$	2×10^{-10}		see text
$Br + BrONO_2 \rightarrow Br_2 + NO_3$	6.7×10^{-11}		11
$Br + O_3 \rightarrow BrO + O_2$	1.2×10^{-12}		2
$Br + NO_3 \rightarrow BrO + NO_2$	1.6×10^{-11}		2
$Br + Br_2O \rightarrow Br_2 + BrO$	2×10^{-10}		14
$BrO + BrO \rightarrow Br_2 + O_2$	5.02×10^{-13}		2
$BrO + BrO \rightarrow Br + Br + O_2$	2.75×10^{-12}		2

[a] Units of cm^3 $molecule^{-1}$ s^{-1}. [b] Calculated (see text).

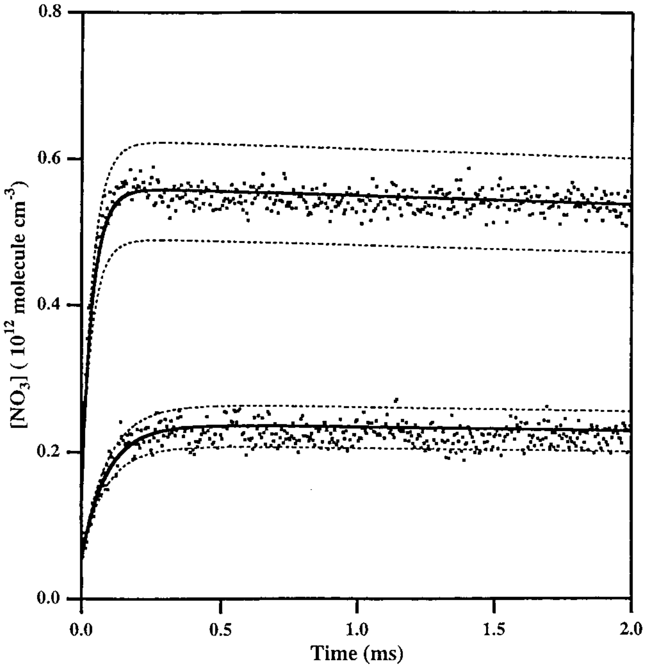

Figure 2. NO_3 concentration profiles measured (dots) following the photolysis of $BrONO_2/N_2$ mixtures at 298 K. The $BrONO_2$ concentrations used were 2.21 and 5.19 × 10^{14} molecule cm^{-3}. The solid lines are the modeled fit (Table 2) using the photolysis laser fluence measured, as described in the text. The dashed lines represent the model using the limits for the O atom yield in $BrONO_2$ photolysis quoted by Soller (0.66 ± 0.15).[1]

In our experiments, the direct photolysis of $BrONO_2$ at 248 nm was unavoidable. NO_3 produced from the photolysis of $BrONO_2$, $[NO_3]_p$ (where subscript p is used to indicate a photolysis product), will appear instantaneously with the photolysis pulse. The contribution of $[NO_3]_p$ to the total concentration of NO_3 is determined by the $[O_3]/[BrONO_2]$ ratio and the NO_3 yield in reaction 1. The $[O_3]/[BrONO_2]$ ratio was varied between measurements and fell between 0.46 and 2.56. Therefore, the initial O atom concentration, $[O]_0$, will be between 20 and 115 times greater than $[NO_3]_p$. As shown in Figure 1, the amount of NO_3 produced by $BrONO_2$ photolysis is small compared to that generated through reaction 1 (the contribution from Br atom reactions is discussed below). The fact that the concentration of NO_3 after reaction 1 has gone to completion, ~600 μs, is significantly greater than $[NO_3]_p$ gives us an early indication that the NO_3 yield from reaction 1 is reasonably high, as expected.

The other $BrONO_2$ photoproducts that need to be accounted for include BrO, Br, and O. The quantum yield for BrO radicals was not measured directly by either Harwood et al.[11] or Soller et al.[1] We have inferred a BrO quantum yield of 0.65 from their measurements of other species. It should be noted that $BrONO_2$ photolysis does not represent the only source of BrO radicals in this system. In fact, reaction 1 will most likely be the major source of BrO in our experiments. The dominant loss process for BrO radicals in our experiments is the self-reaction

$$BrO + BrO \rightarrow Br_2 + O_2 \tag{9a}$$

$$\rightarrow 2Br + O_2 \tag{9b}$$

The generation of Br atoms in reaction 9b will lead to secondary generation of NO_3 via the reaction

$$Br + BrONO_2 \rightarrow Br_2 + NO_3 \tag{10}$$

Harwood et al.[11] have shown the NO_3 yield in reaction 10 to be unity. However, reaction 9 does not greatly influence the interpretation of the NO_3 profiles in our experiments. Reaction 9 occurs on a longer time scale than reaction 1 because of the low BrO radical concentrations (reaction 9 is second-order in BrO radicals) generated and the slower rate coefficients for reaction 9 (see Table 2).

The quantum yields for Br and O atoms from $BrONO_2$ photolysis, 0.38 and 0.66, respectively, will lead to NO_3 formation through reactions 10 and 1. Following the same reasoning presented above for $[NO_3]_p$, the $[O]_0/[O]_p$ ratio will range from 8.8 to 49 for the $[O_3]/[BrONO_2]$ ratios used in our experiments, whereas $[O]_0/[Br]_p$ will range from 15 to 85. Therefore, the contribution of $[O]_p$ to the NO_3 signal through reaction 1 will be at most 11%. The contribution of $[Br]_p$ to the NO_3 signal through reaction 10 will depend on the NO_3 yield in reaction 1 (i.e., it would be a maximum of 7% for a NO_3 yield of one but higher if the yield is less than one). Therefore, unless the NO_3 yield in reaction 1 is significantly less than unity, the photolysis of $BrONO_2$ will not limit the analysis but needs to be included.

Upper limits to the Br_2 and Br_2O impurity levels in the reactor/absorption cell were determined by UV absorption. Br_2O was determined to be <0.5% of the $BrONO_2$ concentration. The rate coefficient for reaction 7 is not known, but the reaction is expected to be slower than the nearly gas kinetic Br atom reaction

$$Br + Br_2O \rightarrow Br_2 + BrO \tag{11}$$

We expect the products of reaction 7 to be two BrO radicals. Therefore, the potential complication from reaction 7 is not through the secondary generation of NO_3, which would occur on a longer time scale than reaction 1, but through the consumption of O atoms. However, even if reaction 7 had a rate coefficient equal to that of reaction 11, 2×10^{-10} cm^3 molecule^{-1} s^{-1}, it would consume <3.5% of the O atoms. In analogy with Cl_2O and its rate coefficients for Cl and O atom reactions, we would expect k_7 to be about a factor of 5 smaller than k_{11}. This would make the upper limit for O atom consumption through reaction 7 negligible in our experiments. For fitting and data analysis purposes, we have taken k_7 to be equal to k_{11}.

The Br_2 impurity level was determined by UV absorption to be <5% of the $BrONO_2$ concentration. The reaction

$$O + Br_2 \rightarrow BrO + Br \tag{12}$$

will affect the O atom loss through reaction 1 and will also lead to rapid formation of NO_3 from the Br atom product through reaction 10. Reaction 12 will lead to <2% loss of O atoms. Fitting calculations were made assuming the maximum Br_2 impurity level.

The fitting results, NO_3 yield, are given in Table 1. The fits reproduced the measured NO_3 profiles within the uncertainties in the initial concentrations, rate coefficients, and laser fluence very well. The fits are shown as the solid lines in Figure 1. The NO_3 yields were independent of the $[O_3]/[BrONO_2]$ ratio, with an average value of 0.95 ± 0.12 for the 12 measurements. The uncertainty is the 2σ precision of the fitted values.

The absolute uncertainty in the reaction yield is determined by the uncertainties in the NO_3 measurements and the laser fluence determination. The uncertainty in the NO_3 measurements appears in the deviations of the individual measurements, as quoted above. The uncertainty in the laser fluence is determined by the uncertainties in the quantities used in eq 6. The uncertainty in the NO_3 yield, $\Phi(NO_3)$, is estimated to be ~15%. Although the uncertainty in the NO_3 absorption cross section contributes to the uncertainty in the absolute laser fluence, it cancels in the product yield analysis. The uncertainty in the absorption cross sections for N_2O_5 in the concentration determination and at the laser photolysis wavelength also nearly cancel, i.e., the relative N_2O_5 absorption cross sections are more accurate than the values at a given wavelength. We estimate the uncertainty in the relative N_2O_5 cross sections to be <3%. Therefore, the accuracy of the laser fluence determination is primarily limited by the accuracy of the NO_3 yield in N_2O_5 photolysis. Although N_2O_5 is well suited as an actinometer for these experiments (direct detection of NO_3), the NO_3 yield in reaction 5 is less than unity. An actinometer with a unit quantum yield would be ideal for our measurements. The uncertainty, ~15%, in the reaction 5 NO_3 yield will translate directly into the uncertainty in the NO_3 yield determination for reaction 1. Therefore, the absolute 2σ uncertainty in our NO_3 yield is taken to be ~25%.

The possible products of reaction 1 were outlined in the Introduction. Only reaction channels 1c, 1e, and 1f would lead to NO_3 production in our experiments. Channels 1e and 1f are indistinguishable in our experiments because BrOO would rapidly decompose to Br + O_2 on a time scale faster than reaction 1. Channel 1c leads to the direct formation of NO_3, whereas channels 1e and 1f would lead to its formation through reaction 10. In our measurements, channels 1e and 1f will manifest themselves as a decrease in the rate of NO_3 formation. A sensitivity analysis of our fits indicates that a 10% yield for channels 1e + 1f would be detectable (taking the rate coefficient for reaction 1 reported by Soller et al.).[1] Therefore, we conclude the yield for channels 1c, 1e, and 1f is 0.95 ± 0.12, with that for channel 1c >0.85 at 298 K.

References and Notes

(1) (a) Soller, R., Ph.D. Dissertation, Georgia Institute of Technology, Atlanta, GA, 1998. (b) Soller, R.; Nicovich J. M.; Wine P. H. *J. Phys. Chem.* **2000**, submitted.

(2) DeMore, W. B.; Sander, S. P.; Goldan, D. M.; Hampson, R. F.; Kurylo, M. J.; Howard, C. J.; Ravishankara, A. R.; Kolb, C. E.; Molina, M. J. *Chemical Kinetics and Photochemical Data for Use in Stratospheric Modeling*; JPL Publication No. 97-4; Jet Propulsion Laboratory: Pasadena, CA, 1997.

(3) Chase, M. W. *J. Phys. Chem. Ref. Data* **1996**, *25*, 1069.

(4) Goldfarb, L.; Harwood, M. H.; Burkholder, J. B.; Ravishankara, A. R. *J. Phys. Chem.* **1998**, *102*, 8556.

(5) Yokelson, R. J.; Burkholder, J. B.; Goldfarb, L.; Fox, R. W.; Gilles, M. K.; Ravishankara, A. R. *J. Phys. Chem.* **1995**, *99*, 13976.

(6) Burkholder, J. B.; Ravishankara, A. R.; Solomon, S. *J. Geophys. Res.* **1995**, *100*, 16793.

(7) Orlando, J. J.; Burkholder, J. B. *J. Phys. Chem.* **1995**, *99*, 1143.

(8) Maric, D.; Burrows, J. P.; Moortgat, G. K. *J. Photochem. Photobiol. A: Chem.* **1994**, *83*, 179.

(9) Yokelson, R. J.; Burkholder, J. B.; Fox, R. W.; Talukdar, R. K.; Ravishankara, A. R. *J. Phys. Chem*. **1994**, *98*, 13144.

(10) Burkholder, J. B.; Ravishankara, A. R. *J. Phys. Chem. A* **2000**, in press.

(11) Harwood, M. H.; Burkholder, J. B.; Ravishankara, A. R. *J. Phys. Chem.* **1998**, *102*, 1309.

(12) Spencer, J. E.; Rowland, F. S. *J. Phys. Chem.* **1978**, *82*, 7.

(13) Nicovich, J. M.; Wine, P. H. *Int. J. Chem. Kinet*. **1990**, 22, 379.

(14) Burkholder, J. B. *Int. J. Chem. Kinet.* **1998**, *30*, 571.